Supporting Information

for

Formation of aminyl radicals on electron attachment to AZT: Abstraction from the sugar phosphate backbone vs. one-electron oxidation of Guanine

by

Amitava Adhikary, Deepti Khanduri, Venkata Pottiboyina, Cory T. Rice, and Michael D. Sevilla*

Department of Chemistry
Oakland University
Rochester, MI 48309

Supporting Information:

Supporting Information S1: Simulation of the experimentally recorded ESR spectra of T(C3')-ND• and T(C3')-NH• shown in Figure 3 in the manuscript.

Supporting Information S2: Studies of electron attachment to 3'-AZT in D_2O at high pD (ca. 12).

Supporting Information S3: Radicals formed after γ-irradiation of a 7.5 M LiCl solution containing 5'-AZT (Figure S3A) at 77 K and subsequent annealing to higher temperatures (Figures S3B to S3D). Also, spectral evidence showing predominant formation of C3'• via intermolecular H-abstraction by T(C5')-ND• in 5'-AZT.

Supporting Information S4: Simulation of the experimentally recorded ESR spectrum of T(C5')-ND• shown in Figure 5A in the manuscript.

Supporting Information S5: Radicals formed after γ-irradiation of a 7.5 M LiCl solution containing 5'-AZG (Figure S5A) at 77 K followed by photo-excitation at 77 K and annealing to 150 K (Figures S5B and S5C).

Complete reference of the reference no. 24 in the text.

Supporting Information S1:

Simulation of the experimentally recorded ESR spectra of T(C3')-ND• and T(C3')-NH• shown in Figure 3:

The parameters used to simulate the experimental spectrum (Green) of T(C3')-ND• (in D_2O, Figure 3A) and the experimental spectrum (Red) of T(C3')-NH• (in H_2O, Figure 3B) are mentioned below.

For simulation of the experimentally recorded spectrum of T(C3')-ND• (Green), the following parameters were used: A(Hβ) 41.0 G, A(N) [37.5,0,0] G, lineshape function Lorentzian/Gaussian 1.00, line-width 17.0 G (Isotropic), g [2.0020, 2.0043, 2.0043]. To simulate the experimentally recorded spectrum of T(C3')-NH• (red), we have employed the following parameters: A(βH) 41.0 G, A(N) [37.5,0,0]G, A(αH) (-39.5, 0.4, -28) G, Lorentzian/Gaussian 1.00, line-width 17.0 G (isotropic), g [2.0020, 2.0043, 2.0043].

Supporting Information S2:
Studies of electron attachment to 3'-AZT in D_2O at high pD (ca. 12):

Figure S2A represents the ESR spectrum of the radicals formed in 3'-AZT after electron attachment in a homogeneous glassy solution of 7.5 M LiCl/D_2O at pD ca. 12 after subtraction of the D• and $Cl_2•^-$ spectra from the experimentally recorded spectrum at 77 K. For comparison, the ESR spectrum (blue) of the radicals formed in 3'-AZT after electron attachment at the native pD (ca. 5) of the in a homogeneous glassy solution of 7.5 M LiCl/D_2O (spectrum 2A in the manuscript) is shown underneath. This blue spectrum is also found after subtraction of the D• and $Cl_2•^-$ spectra from the experimentally recorded spectrum at 77 K. In Figure S2B, the first derivative ESR spectrum (black) found by subtracting the D• and $Cl_2•^-$ spectra from the experimental spectrum recorded after visible illumination of this sample by a photoflood lamp at 77 K for 15 minutes to remove the thymine anion radical is shown. This spectrum shown in Figure S2B matches closely with the ESR spectrum (blue) of **the neutral aminyl radical (T(C3')-ND•)** found in 3'-AZT (spectrum 2B in the manuscript) in a similarly treated sample. Thus even at pD ca. 12, the protonation of the nitrene anion radical (T(C3')-N•$^-$) leading to the formation of the neutral aminyl radical (T(C3')-ND•) (reaction 3) from the solvent (D_2O) is complete at 77 K.

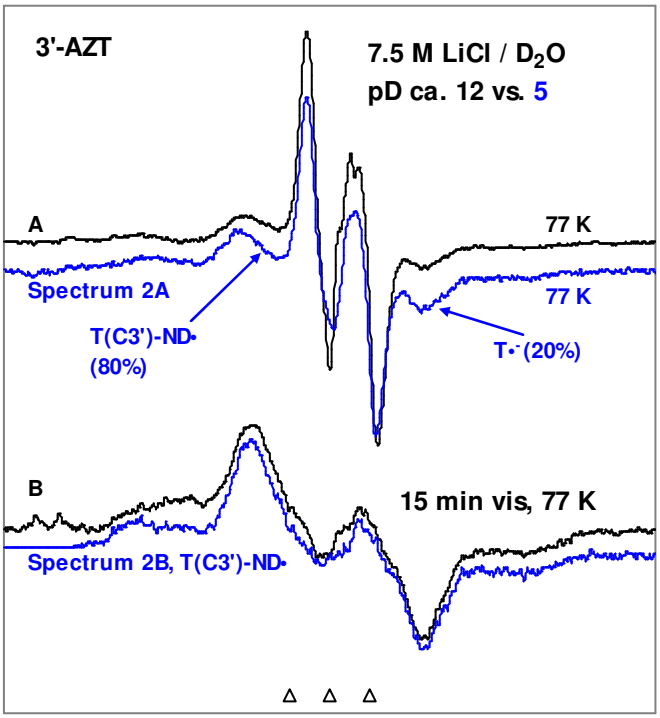

Figure S2. All the spectra shown in A and B are found after subtraction of the D• and $Cl_2•^-$ spectra from the experimentally recorded spectrum at 77 K. (A) ESR spectrum for 3'-AZT after one-electron addition at 77 K at pD ca. 12 (black) and at the native pD (*ca.* 5) (blue, spectrum 2A in the manuscript) in the homogeneous glassy solution of 7.5 *M* LiCl in D_2O. (B) After visible illumination of the sample at pD ca. 12 (black) by using a photoflood lamp at 77 K for 15 minutes to remove the thymine anion radical by photoejection of the excess electron. For comparison, ESR spectrum (blue) of the neutral aminyl radical (T(C3')-ND•) found in 3'-AZT at the native pD (ca. 5) of the 7.5 M LiCl/D_2O (spectrum 2B in the manuscript) under identical condition is shown. The close match between these two spectra shows the formation of the neutral aminyl radical (T(C3')-ND•) in 3'-AZT even at pD ca. 12.

Supporting Information S3:

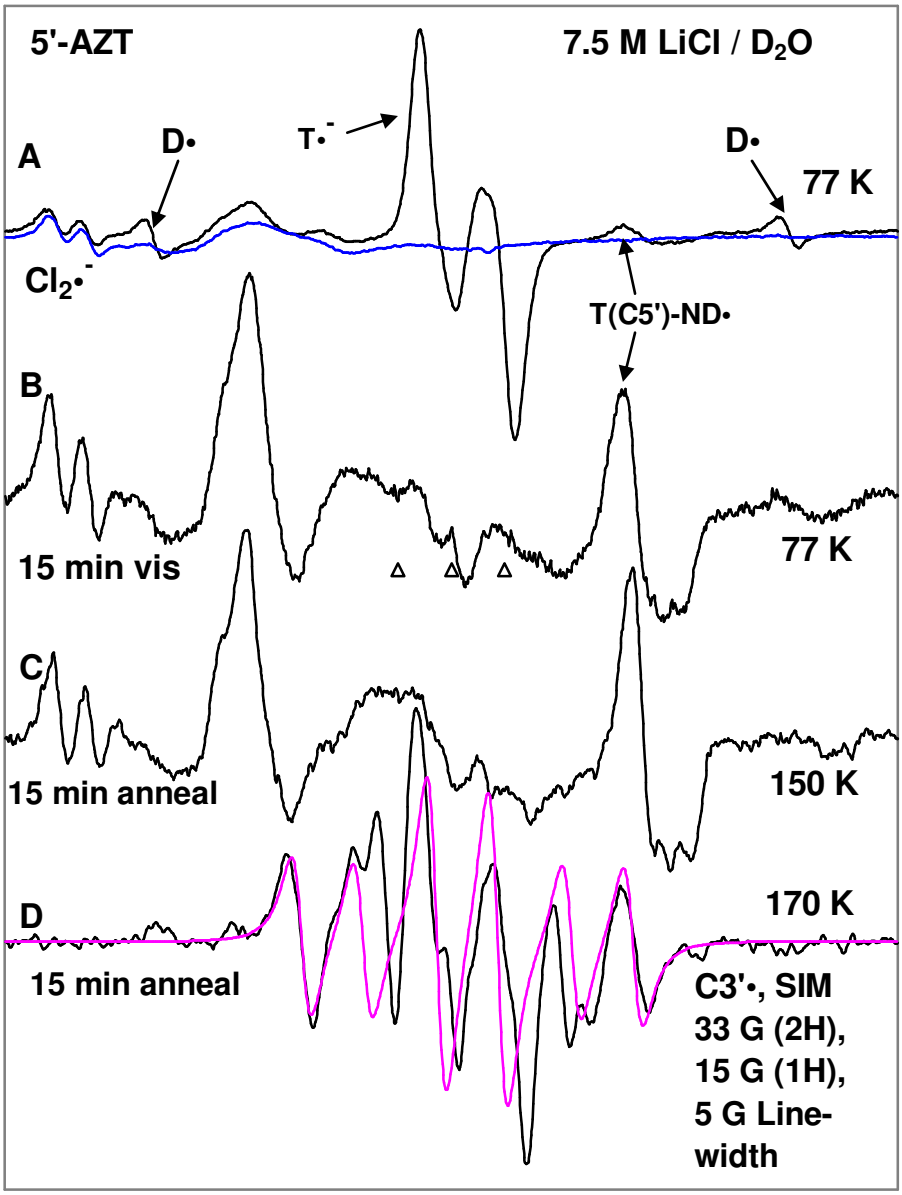

Figure S3. ESR spectrum (A) (black) for 5'-AZT recorded at 77 K after one-electron addition at 77 K at the native pD (*ca.* 5) of the homogeneous glassy solution of 7.5 *M* LiCl in D_2O. For comparison, the ESR spectrum of $Cl_2•^-$ in D_2O (7.5 M LiCl) (blue) has been superimposed on it. (B) ESR spectrum (black) recorded at 77 K after visible illumination of the sample by using a photoflood lamp at 77 K for 15 minutes to remove the thymine anion radical by photoejection of the excess electron. (C) ESR spectrum (black) of this sample after subsequent annealing in the dark at (C) 150 K for 15 min. (D) ESR spectrum of this

sample after subsequent annealing of this sample in the dark at 170 K for 15 min. The simulated spectrum (violet) of the C3'• with the parameters (33 G(2 βH), 15 G (1βH), 5 G line-width match well the line components of spectrum (D) thereby establishing that in 5'-AZT, C3'• is mainly produced via intermolecular H-abstraction by T(C5')-ND•.

Supporting Information S4:

Simulation of the experimentally recorded ESR spectrum of T(C5')-ND• shown in Figure 5A

The spectrum of T(C5')-ND• in Figure 5A has been simulated (blue color) and the simulated spectrum is superimposed on the experimentally observed spectrum (green) for comparison.

We note here that a variety of conformations for the T(C5')-ND• exist (see theoretical studies in the manuscript) which give a variety of couplings for the two β-protons on the C5' carbon. However the sum of the two β-proton couplings is relatively constant at 91 G and this give the appearance of the sharp outer peaks and the broadened inner two components. We have taken several sets of the two β-couplings (e.g., (50, 41) G; (60, 31) G; (70, 21) G)) so that the sum of the two β-proton couplings is more or less constant at ca. 91 G along with the same anisotropic Nitrogen hyperfine couplings ($A_{\|}$, of *ca.* 43 G, $A_{\perp} = 0$) with $g_{\|} = 2.0020$ and $g_{\perp}=2.0043$. With these parameters, and taking the linewidths as (15, 12, 12) G, we have simulated separate spectra and simply added them together. The addition is shown simulated spectrum (blue) superimposed on the experimentally recorded (green) first derivative spectrum shown in Figure 5A in the manuscript.

The similarity between the experimentally recorded (green) spectrum of T(C5')-ND• (Figure 5A) with the simulated (blue) spectra in Figure 5A point towards the existence of various conformations of T(C5')-ND• and hence of T(C5')-NH• even at 77 K and the theoretical results pertaining to the various conformations of T(C5')-NH• (or T(C5')-ND•) are shown in section 2.2 in the manuscript.

Supporting Information S5:

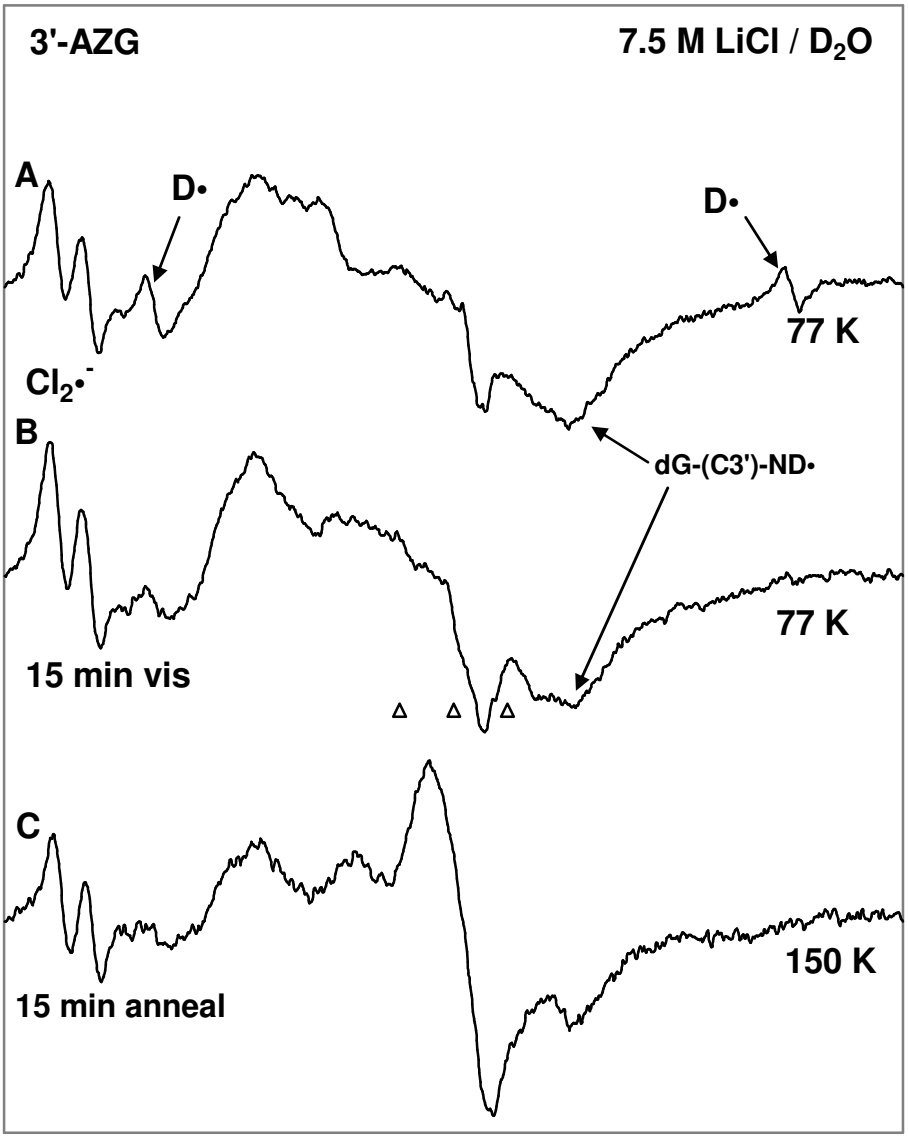

Figure S5. ESR spectrum (A) (black) for 3'-AZG recorded at 77 K after one-electron addition at 77 K at the native pD (*ca.* 5) of the homogeneous glassy solution of 7.5 *M* LiCl in D_2O. For comparison, the ESR spectrum of $Cl_2\bullet^-$ in D_2O (7.5 M LiCl) (blue) has been superimposed on it. (B) ESR spectrum (black) recorded at 77 K after visible illumination of the sample by using a photoflood lamp at 77 K for 15 minutes. (C) ESR spectrum (black) of this sample after subsequent annealing in the dark at (C) 150 K for 15 min.

Complete reference of the reference no. 24 in the text:

30. Frisch, M. J.; Trucks, G. W.; Schlegel, H. B.; Scuseria, G. E.; Robb, M. A.; Cheeseman, J. R.; Montgomery, J. A., Jr.; Vreven, T.; Kudin, K. N.; Burant, J. C.; Millam, J. M.; Iyengar, S. S.; Tomasi, J.; Barone, V.; Mennucci, B.; Cossi, M.; Scalmani, G.; Rega, N.; Petersson, G. A.; Nakatsuji, H.; Hada, M.; Ehara, M.; Toyota, K.; Fukuda, R.; Hasegawa, J.; Ishida, M.; Nakajima, T.; Honda, Y.; Kitao, O.; Nakai, H.; Klene, M.; Li, X.; Knox, J. E.; Hratchian, H. P.; Cross, J. B.; Adamo, C.; Jaramillo, J.; Gomperts, R.; Stratmann, R. E.; Yazyev, O.; Austin, A. J.; Cammi, R.; Pomelli, C.; Ochterski, J. W.; Ayala, P. Y.; Morokuma, K.; Voth, G. A.; Salvador, P.; Dannenberg, J. J.; Zakrzewski, V. G.; Dapprich, S.; Daniels, A. D.; Strain, M. C.; Farkas, O.; Malick, D. K.; Rabuck, A. D.; Raghavachari, K.; Foresman, J. B.; Ortiz, J. V.; Cui, Q.; Baboul, A. G.;Clifford, S.; Cioslowski, J.; Stefanov, B. B.; Liu, G.; Liashenko, A.; Piskorz, P.; Komaromi, I.; Martin, R. L.; Fox, D. J.; Keith, T.; Al-Laham, M. A.; Peng, C. Y.; Nanayakkara, A.; Challacombe, M.; Gill, P. M. W.; Johnson, B.; Chen, W.; Wong, M. W.; Gonzalez, C.; Pople, J. A. Gaussian03, Revision B.04; Gaussian, Inc.: Pittsburgh, PA, 2003.